Enhanced Smith-Purcell radiation based on quasibound states in the continuum in dimers aligned in a chain

D. Yu. Sergeeva and A. A. Tishchenko[*]

National Research Nuclear University "MEPhI," 115409, Moscow, Russia
and Laboratory of Radiation Physics, Belgorod National Research University, 308015, Belgorod, Russia

In this work we theoretically investigate the radiation from electrons passing along a periodic chain of dimers—the particles consisting of two coupled subwavelength parts. High-quality resonances can be excited in dimers due to interaction between the constituent particles, making quasibound states in the continuum. We show that at the resonant frequencies, the intensity of Smith-Purcell radiation increases sharply. Although numerical analysis is performed for the dimers consisting of two equal-coupled particles, the theory constructed is valid for more general binary objects consisting of two different subwavelength-coupled particles of arbitrary form and dielectric properties, and we have formulated the analytical conditions describing this effect. We prove that there is a wide range of the parameters for which Smith-Purcell radiation can be boosted by up to two orders of magnitude. Apparently, the effect can be even stronger with an appropriate choice of parameters. A resonant mechanism of enhancement of Smith-Purcell radiation paves the way to the novel and very effective radiation source based on metasurfaces made of resonant elements.

I. INTRODUCTION

Bound states in the continuum (BICs) are known from the pioneering research of von Neuman and Wigner [1]. Their work, being for that moment a pure mathematical abstraction, can be called a play of the intellect: in quantum mechanics, to choose the form of the potential so that the eigenmodes of the energy spectrum would lay in the region of the continuous spectrum of the propagating modes of the neighboring space. That is, the bound states must be inside a zone forbidden to them. BICs do not interact with any of states of the continuum spectrum (i.e., cannot emit or absorb any wave). Such states characterized by an infinite quality factor cannot be observed. In reality, however, the "spoiled" BICs, or quasi-BICs, can describe high-quality resonances in a continuous spectrum. Since BICs (and quasi-BICs) have a wave nature, they take place not only in quantum mechanics, but also in photonics [2–4] and other areas of physics [4–6].

Recently, BICs became the object of study in physics of radiation by free electrons, where they are considered a way of increasing of radiation intensity. In general, the standard way to increase the intensity of radiation from a beam of N_e electrons is to implement a coherent mode so that the radiation intensity will be proportional to N_e^2. The most famous example of this kind is free-electron lasers (FELs). Today, the European x-ray FEL and the FEL of the Linac coherent light source are the brightest radiation sources created by humankind. However, the question arises: are there other mechanisms of radiation amplification in addition to the coherent one? And here, the idea of using quasi-BICs opens new horizons.

Back in 1994, Zhevago and Glebov [7] semiqualitatively considered the problem of radiation amplification for a single particle in the form of a protrusion—a hemisphere on the surface of a metal. In Ref. [8], the effect of amplification of the field acting on average on an individual film particle (the so-called local field) surrounded by similar particles was considered. It was demonstrated that the amplification caused by the local field effect can be of almost two orders of magnitude. Actually, though in Refs. [7] and [8] the term BIC was not used, high-quality resonances were considered there, and are now considered in terms of quasi-BICs.

The next step has been made just recently. Yang *et al.* [9] demonstrated that the contribution of quasi-BICs can be so significant that nonrelativistic electrons can achieve stronger Smith-Purcell radiation (SPR) than relativistic ones (they even called it "a new operation regime"). Song *et al.* [10] came to a similar conclusion about slow electrons when considering Cherenkov radiation [10]. In a recent series of papers, Chen *et al.* also considered the effect of enhancement of SPR near quasi-BIC resonances, both for plain [11] and cylindrical gratings [12,13]. Similar to other modern papers on this problem (with the exception of Ref. [9]), research is being conducted using computer simulations with minimal (quantitative) theoretical basis, and for nonrelativistic electrons only.

In this work, we propose a new type of a grating for generating SPR that can produce more intense radiation due to resonant interaction between grating elements inside small two-particle clusters: dimers. The grating consists of pairs of coupled small particles that are arranged periodically in a plane (see Fig. 1). The particles can be either metallic or dielectric to avoid strong absorption by metals.

The Coulomb field of a moving electron acts on the grating exiting SPR. By fabricating the grating in a special way, it becomes possible to make the particles interact at a frequency
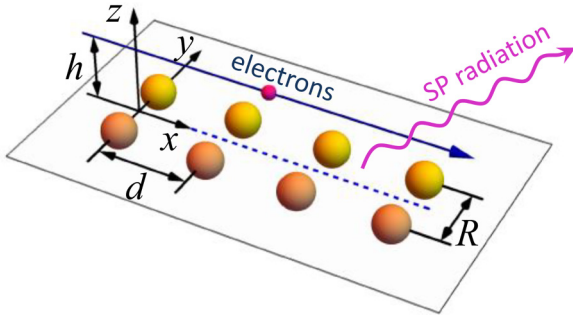
---

*tishchenko@mephi.ru

FIG. 1. Pairs of coupled particles arrange a grating that radiates while an electron moves along it.

that coincides with the SPR diffraction order. The resulting enhancement of a separate diffraction order can reach 10 to 100 times in the presence of a resonance. Here we call the pairs of coupled particles dimers. The increase in intensity is achieved because of the superposition of radiation from a grating and resonant effects caused by interactions in a dimer.

II. RADIATION FROM A BINARY DIMER CONSISTING OF TWO DIFFERENT PARTICLES

When an electron moves near a couple of small particles, the small particles emit radiation due to induced dynamic polarization of the material caused by the Coulomb field. The smallness means that the size of the particles r_1, r_2 is much less than the wavelength of radiation λ:

$$r_1, r_2 \ll \lambda. \tag{1}$$

Two particles in such a dimer interact not only with the electron, but also with each other. The layout of generation of the radiation by an electron from a dimer is shown in Fig. 2. The coordinate system is chosen so that an electron moves along the x-axis at a constant distance h from the plane $z = 0$, in which the dimer is placed. Here we designate the parameters of the particle having the polarizability $\alpha_1(\omega)$ with the index 1, and the parameters related to the particle having the polarizability $\alpha_2(\omega)$ with the index 2. Vectors $\mathbf{R}_1$ and $\mathbf{R}_2$ define the positions of the particles.
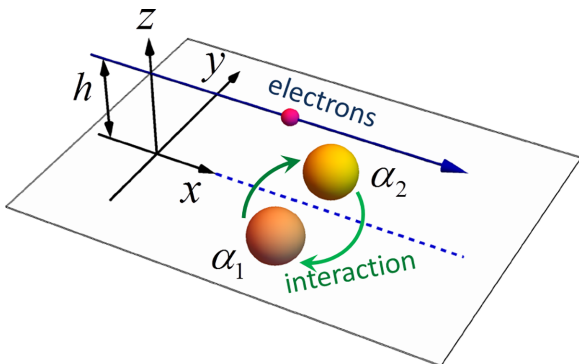

FIG. 2. An electron moving close to a dimer of coupled particles emits radiation. The green arrows indicate the interaction between particles.

This section is based on the results from Ref. [14], and here we give the final formulas only for the convenience of the reader. The field of radiation of a dimer in Fig. 2 is

$$
\begin{aligned}
\mathbf{E}_d(\mathbf{r}, \omega) = &-\alpha_1(\omega)\frac{e^{ikr}}{r}e^{-i\mathbf{k}\cdot\mathbf{R}_1}(\mathbf{k} \times \{\mathbf{k} \times [\mathbf{E}_0(\mathbf{R}_1, \omega) \\
&+ \mathbf{E}_2(\mathbf{R}_1, \omega)]\}) - \alpha_2\frac{e^{ikr}}{r}e^{-i\mathbf{k}\cdot\mathbf{R}_2}(\mathbf{k} \times \{\mathbf{k} \\
&\times [\mathbf{E}_0(\mathbf{R}_2, \omega) + \mathbf{E}_1(\mathbf{R}_2, \omega)]\}),
\end{aligned} \tag{2}
$$

where r is the distance to the point of observation; $\mathbf{k} = \mathbf{n}\omega/c$ is the wavevector, with ω being the radiation frequency, c being the speed of light in vacuum; and $\mathbf{n}$ being the unit wavevector. $\mathbf{E}_0$ is the Coulomb field of the moving electron:

$$
\mathbf{E}_0(\mathbf{r}, \omega) = -\frac{ie}{\pi v}e^{i\frac{\omega}{v}x}\frac{\omega}{v\gamma}\left[\frac{1}{\gamma}K_0\left(\frac{\omega}{v\gamma}L\right)\mathbf{e}_x + i\frac{\mathbf{L}}{L}K_1\left(\frac{\omega}{v\gamma}L\right)\right], \tag{3}
$$

where $\mathbf{L} = y\mathbf{e}_y - h\mathbf{e}_z$, $\mathbf{e}_y$ and $\mathbf{e}_z$ are the base vectors, K_0 and K_1 are the modified Bessel function of the zero and the first orders, e is the electron charge, $\mathbf{v}$ is its velocity, and γ is the Lorentz factor of the electron. Note that Eq. (3) is not general. It is correct in the plane $z = 0$, as, indicated earlier, the dimer, including its constituent particles, lays in the plane $z = 0$. The field $\mathbf{E}_1(\mathbf{R}_2, \omega)$ [or $\mathbf{E}_2(\mathbf{R}_1, \omega)$] is the field of radiation emitted by the first (or second) particle at the point $\mathbf{R}_2$ (or $\mathbf{R}_1$). The explicit forms of the sth component for these fields read

$$
\begin{aligned}
E_{2s}(\mathbf{R}_1, \omega) = &-e^{iRk}\alpha_2(\omega)V^{-1}t_{sj}^{(1)}E_{0j}(\mathbf{R}_2, \omega) \\
&+ e^{2iRk}\alpha_1(\omega)\alpha_2(\omega)V^{-1}t_{sj}^{(2)}E_{0j}(\mathbf{R}_1, \omega)
\end{aligned} \tag{4}
$$

and

$$
\begin{aligned}
E_{1s}(\mathbf{R}_2, \omega) = &-e^{iRk}\alpha_1(\omega)V^{-1}t_{sj}^{(1)}E_{0j}(\mathbf{R}_1, \omega) \\
&+ e^{2iRk}\alpha_1(\omega)\alpha_2(\omega)V^{-1}t_{sj}^{(2)}E_{0j}(\mathbf{R}_2, \omega),
\end{aligned} \tag{5}
$$

where we have designated

$$
t_{sj}^{(1)} = B\delta_{sj} - \frac{\alpha_1(\omega)\alpha_2(\omega)e^{2iRk}AB(A+B) + A}{W}\frac{R_sR_j}{R^2}, \tag{6}
$$

$$
t_{sj}^{(2)} = B^2\delta_{sj} - \frac{A(A+2B)}{W}\frac{R_sR_j}{R^2}, \tag{7}
$$

$$
V = 1 - \alpha_1(\omega)\alpha_2(\omega)e^{2iRk}B^2, \tag{8}
$$

$$
W = \alpha_1(\omega)\alpha_2(\omega)e^{2iRk}(A+B)^2 - 1, \tag{9}
$$

$$
A = (k^2R^2 + 3ikR - 3)/R^3, \tag{10}
$$

and

$$
B = -(k^2R^2 + ikR - 1)/R^3, \tag{11}
$$

where $R \equiv |\mathbf{R}| = |\mathbf{R}_2 - \mathbf{R}_1|$ and δ_{sj} is the Kronecker delta. The distance R between the particles is the parameter that most determines the interaction and, consequently, the resonant effects.

III. FIELD OF RADIATION FROM A FLAT ARRAY

Being periodically placed along the electron trajectory, the identical pairs of coupled particles arrange a grating (see Fig. 1).

At far distances from the, grating the total field of radiation $\mathbf{E}(\mathbf{r}, \omega)$ is defined by the Fourier-transformed total current density $\mathbf{j}(\mathbf{k}, \omega)$:

$$\mathbf{E}(\mathbf{r}, \omega) = \frac{i(2\pi)^3}{\omega} \frac{e^{ikr}}{r} \{k^2 \mathbf{j}(\mathbf{k}, \omega) - \mathbf{k}[\mathbf{k} \cdot \mathbf{j}(\mathbf{k}, \omega)]\}. \quad (12)$$

According to the superposition principle, the total radiation field is the sum of the radiation fields from every single particle. So, the grating of dimers can be considered two chains along the trajectory in which the particles with the same order number interact. This means that the total current density is a sum of current densities associated with each chain,

$$\mathbf{j}(\mathbf{k}, \omega) = -\frac{i\omega}{(2\pi)^3} \sum_{m=0}^{N-1} \mathbf{p}(\mathbf{R}_1 + dm\mathbf{e}_x, \omega) e^{-i\mathbf{k} \cdot \mathbf{R}_1} e^{-idmk_x}$$
$$- \frac{i\omega}{(2\pi)^3} \sum_{m=0}^{N-1} \mathbf{p}(\mathbf{R}_2 + dm\mathbf{e}_x, \omega) e^{-i\mathbf{k} \cdot \mathbf{R}_2} e^{-idmk_x}, \quad (13)$$

where N is the number of dimers in the grating or the number of particles in a chain, m is the order number of a particle in a chain, d is the period of the grating, $\mathbf{p}$ is a dipole moment induced in a particle, and $\mathbf{e}_x$ is the basis vector. The dipole moment of a particle is defined by the Coulomb field of the moving electron and the field of radiation from the particle with the same order number from another chain:

$$\mathbf{p}(\mathbf{R}_1 + dm\mathbf{e}_x, \omega) = \alpha_1(\omega)\mathbf{E}_0(\mathbf{R}_1 + dm\mathbf{e}_x, \omega)$$
$$+ \alpha_1(\omega)\mathbf{E}_2(\mathbf{R}_1 + dm\mathbf{e}_x, \omega). \quad (14)$$

The formula for $\mathbf{p}(\mathbf{R}_2 + dm\mathbf{e}_x, \omega)$ is written in a similar way. Then, the problem of obtaining $\mathbf{E}_{2,1}(\mathbf{R}_{1,2} + dm\mathbf{e}_x, \omega)$ is solved in the same way as it was done in Sec. II, taking into account $dm\mathbf{e}_x$ in positions of the particles. The result is

$$\mathbf{E}_1(\mathbf{R}_2 + dm\mathbf{e}_x, \omega) = \mathbf{E}_1(\mathbf{R}_2, \omega) \exp(idm\omega/v),$$
$$\mathbf{E}_2(\mathbf{R}_1 + dm\mathbf{e}_x, \omega) = \mathbf{E}_2(\mathbf{R}_1, \omega) \exp(idm\omega/v). \quad (15)$$

Using Eqs. (12)–(15) we obtain the total field of radiation in the form

$$\mathbf{E}(\mathbf{r}, \omega) = \mathbf{E}_d(\mathbf{r}, \omega) \sum_{m=1}^{N} \exp\left[i\left(\frac{\omega}{v} - k_x\right)dm\right], \quad (16)$$

where $\mathbf{E}_d(\mathbf{r}, \omega)$ is the field of radiation from a single dimer defined by Eq. (2).

IV. GEOMETRICAL APPROACH

There is another way to calculate the radiation field of a grating consisting of dimers. Knowing the radiation field of a pair of interacting particles [Eq. (2)], it is possible to use the geometric approach, which we briefly describe here.

As the field of radiation from each pair is the same, the total field of radiation is a sum of fields from all pairs, taking into account the phase shift:

$$\Delta = \mathbf{k} \cdot \Delta\mathbf{r} - \omega\Delta t. \quad (17)$$

Here, $\Delta\mathbf{r}$ is the vector defining the difference in positions of pairs; when the electron moves along the periodicity of the grating, it is $\Delta\mathbf{r} = d\mathbf{e}_x$, Δt defines the time of delay in the moments of radiation, i.e., it is $\Delta t = \Delta r/v = d/v$, which gives us

$$\Delta = d\frac{\omega}{c}(n_x - \beta^{-1}), \quad (18)$$

where $\beta = v/c$ and n_x is the component of the unit wavevector $\mathbf{n}$. The total field of radiation is defined as

$$\mathbf{E}(\mathbf{r}, \omega) = \sum_{m=1}^{N} \mathbf{E}_d(\mathbf{r}, \omega) e^{-i(m-1)\Delta}, \quad (19)$$

which exactly coincides with Eq. (16). Meanwhile, Eqs. (15), (16), and (19) are in complete agreement with the Floquet theorem.

V. RESONANT CONDITIONS

Knowing the total field of radiation at a far distance, we can calculate the energy radiated per unit solid angle per unit angular frequency:

$$\frac{dW(\mathbf{n}, \omega)}{d\omega d\Omega} = cr^2 |\mathbf{E}(\mathbf{r}, \omega)|^2. \quad (20)$$

Or, in the considered case

$$\frac{dW(\mathbf{n}, \omega)}{d\omega d\Omega} = \frac{c}{|V|^2} F |[\mathbf{k} \times (\mathbf{k} \times \mathbf{P})]|^2, \quad (21)$$

where

$$F = \frac{\sin^2\left[N\frac{d}{2}\left(\frac{\omega}{v} - k_x\right)\right]}{\sin^2\left[\frac{d}{2}\left(\frac{\omega}{v} - k_x\right)\right]}, \quad (22)$$

$$\mathbf{P} = \alpha_1(\omega)T_2\mathbf{E}_0(\mathbf{R}_1, \omega) + \alpha_2(\omega)T_1\mathbf{E}_0(\mathbf{R}_2, \omega)$$
$$+ \frac{\alpha_1(\omega)\alpha_2(\omega)A}{W} e^{iRk} \frac{\mathbf{R}}{R^2} \{[T_2 - \alpha_2(\omega)e^{iRk}T_1(A+B)]$$
$$\times (\mathbf{R} \cdot \mathbf{E}_0(\mathbf{R}_2, \omega)) + [T_1 - \alpha_1(\omega)e^{iRk}T_2(A+B)]$$
$$\times (\mathbf{R} \cdot \mathbf{E}_0(\mathbf{R}_1, \omega))\}, \quad (23)$$

$$T_1 = e^{-i\mathbf{k}\mathbf{R}_2} - \alpha_1(\omega)e^{-i\mathbf{k}\mathbf{R}_1}e^{iRk}B,$$
$$T_2 = e^{-i\mathbf{k}\mathbf{R}_1} - \alpha_2(\omega)e^{-i\mathbf{k}\mathbf{R}_2}e^{iRk}B, \quad (24)$$

where denominators V and W are defined by Eqs. (8) and (9), respectively. The formula for the spectral-angular distribution of radiation from noninteracting particles can easily be obtained from Eqs. (21)–(24), provided $V = 1$ and $W = -1$, which formally occurs if $A = B = 0$.

To obtain the ratio of the squared sines in Eq. (22), we use the formula for the finite sum of a geometric progression. This ratio gives a common dispersion relation of SPR,

$$\lambda l = d(\beta^{-1} - \cos\theta), \quad (25)$$

where θ is the angle between the wavevector $\mathbf{k}$, and the electron's trajectory, i.e., $n_x = \cos\theta$, l is a positive integer.

From the denominators $|V|^2$ and $|W|^2$ in Eq. (21), there follow the conditions defining the interaction between the

particles in a dimer:

$$|V|^2 = |1 - \alpha_1(\omega)\alpha_2(\omega)e^{2iRk}B^2|^2 = \min \qquad (26)$$

and

$$|W|^2 = |1 - \alpha_1(\omega)\alpha_2(\omega)e^{2iRk}(A+B)^2|^2 = \min . \qquad (27)$$

Note that $|V|^2$ and $|W|^2$ in the right parts of Eqs. (26) and (27) are minimal but never equal zero. These conditions contain the wavelength of radiation through k and do not contain the Lorentz factor of the electron and the angles of radiation. The latter does not seem evident because a dimer is not symmetric and it has a preferential direction: along a line connecting the centers of two particles. However, this is a consequence of measuring the radiation in a far zone, where a dimer looks like a point particle.

VI. POLARIZABILITY

For further analysis, the polarizability is taken in the Raleigh form correct within long-wave approximation [15],

$$\alpha_{1,2}(\omega) = r_{1,2}^3 \frac{\varepsilon(\omega) - 1}{\varepsilon(\omega) + 2}, \qquad (28)$$

where $\varepsilon(\omega) = \varepsilon'(\omega) + i\varepsilon''(\omega)$ is a function of dielectric permittivity of the particles' material. The most known form for $\varepsilon(\omega)$ in the long-wave approximation is the Drude model, which reads

$$\varepsilon(\omega) = 1 - \frac{\omega_p^2}{\omega(\omega + i\Gamma)}, \qquad (29)$$

where ω_p is the plasma (or Langmuir, or plasmon) frequency and Γ is the damping frequency characterizing the width, or inverse relaxation time characterizing excited states in the conduction band, i.e., plasmons [16]. The parameters ω_p and Γ are phenomenological. For example, the complex function of permittivity in the form of the Drude model is determined experimentally in the terahertz range in [17,18].

THz frequencies are far from the plasma frequency defined earlier. However, it is known that the Drude model can overestimate absorption in the profile wings, see Ref. [19] and references there. Consequently, there are some suggestions on wing correction in the Drude model [18]. Yet the corrections touch the amplitude but not the functional behavior. On the other hand, $\varepsilon(\omega)$ in our formulas presents only in the polarizability, which is just a coefficient that we can use to analyze the unmodified Drude model.

If the particles are metal, their properties are mainly determined by conductivity electrons, and the contribution of the electrons bound near ion cores [16] is usually considered to be insignificant [20]. Yet even for metals, the part of dielectric function related to the ion cores and bound electrons can sometimes contribute much. For example, for silver, this high contribution at 4 eV leads to shift in frequency of surface plasmons [16,20]. A similar situation occurs for copper at 2 eV, but the contribution is not high enough to shift the frequency of surface plasmons. In any case, considering the THz range, we can use Eq. (29), as mentioned discrepancies are at higher frequencies. Besides, there is some experimental

research where the Drude model was proved to be suitable for the far-infrared THz range [17,18,21–23].

VII. ENHANCEMENT OF RADIATION

For further analysis, it is useful to note two points. First, as typical values of ω_p are 5 to 10 eV, which exceeds considerably the frequencies in THz range, the effects discussed next weakly depend on the material. That is, using the example of a concrete metal, we can demonstrate all the general characteristics of the radiation. For example, we can use the parameters for copper: 13 eV for plasma frequency ω_p and 0.25 meV for Γ. These parameters are extracted from a comparison of Eq. (29) with experimental data [17] and fit well, at least at 0.5 to 3 THz.

Second, between the two conditions in Eqs. (26) and (27), the first one is usually more influential as it comes from a denominator common for all the summands in the field of radiation, while the second one is caused only by the denominator in the last summand in Eq. (23). Besides, Eq. (26) can be simplified as

$$|V|^2 = (a_{\mathrm{Re}} - 1)^2 + a_{\mathrm{Im}}^2 + 4\sin(kR)[a_{\mathrm{Re}}\sin(kR) + a_{\mathrm{Im}}\cos(kR)], \qquad (30)$$

with a_{Re} and a_{Im} being the real and imaginary parts of $\alpha_1(\omega)\alpha_2(\omega)B^2$. This form shows that $|V|^{-2}$ is an oscillating function of the wavelength of radiation and the distance R. For $kR \gg 1$, the function $|V|^{-2}$ goes to unity, which means that SPR will not be enhanced.

The value $|V|^{-2}$ as a function of R for fixed wavelength is shown in Fig. 3. The axes originate from the value of the diameter of a particle rather than zero, as two particles are farther apart from each other than at the particle's diameter.

Let us suppose that the oscillation of $|V|^{-2}$ is defined mostly by $\sin(kR)$. Then, $|V|^{-2}$ should have its maxima close to $kR = \pi s$, where s is an integer. For the parameters of Fig. 3(a), we obtain R_s: $R_2 = 533.4$ μm, $R_3 = 800.1$ μm, $R_4 = 1066.8$ μm, and so on. These values are close to the positions of the maxima in Fig. 3, so for a rough estimation, we can use this assumption.

To estimate an enhancement of radiation, we should choose the reference grating. Let this grating be a chain of the same number N of single particles and with the same period d. To keep the symmetry of the problem, let the particles be placed in the same plane straight under the electron trajectory, i.e., have their positions defined by $\tilde{\mathbf{R}}_m = (m-1)d\mathbf{e}_x$, with $m = 1, ..., N$. Placing the particles this way, we change the distance between the particle and the electron. Actually, for a reference grating, this distance is h, while for the grating of dimers, it is $h_{\mathrm{eff}} = \sqrt{h^2 + (R/2)^2} > h$. This fact leads to changing the radiation intensity.

To eliminate this effect of impact parameter, we keep the inequality $R/2 \ll h$ satisfied for further analysis. Note that this inequality is useful for comparison and does not restrict the generality of the theory. Also, as the total intensity of the radiation is proportional to the particle's volume, the particles of the reference grating must have doubled in volume to keep the same volume of the radiating material. This grating is shown in Fig. 4. Getting ahead, we note that such a reference
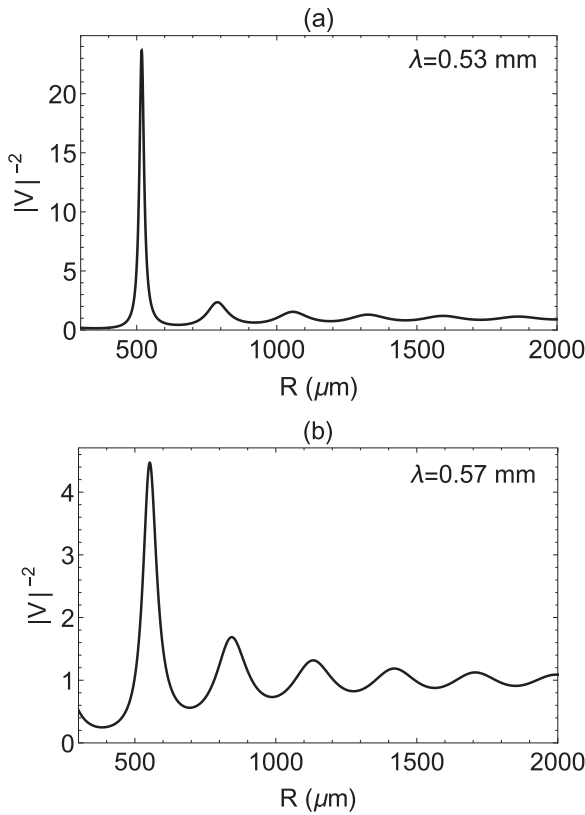
FIG. 3. The value $|V|^{-2}$ as a function of R, which is the distance between two identical copper particles with a radius of 150 μm forming a dimer. Here, (a) $\lambda = 0.53$ mm and (b) $\lambda = 0.57$ mm.

grating is equivalent to the grating of dimers without taking into account interaction between the particles, and all the distributions of these gratings are the same.

Figure 5 shows the wavelength dependence of the spectral-angular distribution of SPR for two gratings: a chain of dimers consisted of two interacting particles (red curves) and the reference grating (black curves) for different parameters. In Fig. 5(a), the black curve is multiplied by a factor of 40. A doubling of the volume is required to keep the amount of radiating material constant. Choosing the distance between two particles in a dimer according to Eqs. (25) and (26), it becomes possible to enhance a certain diffraction order of SPR due to the particles' interaction. For the parameters in Fig. 5(a), the second diffraction order becomes 81.7 times
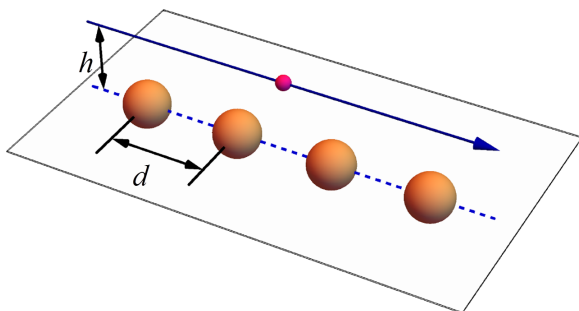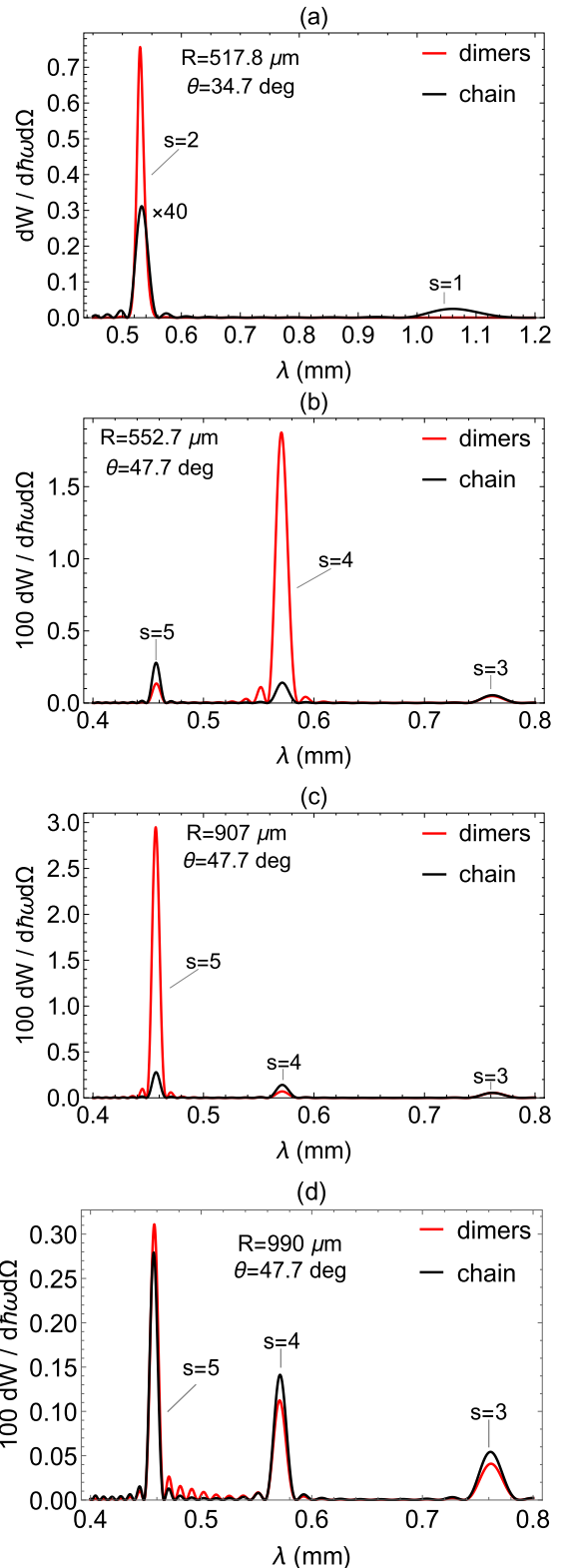

FIG. 4. The reference grating.

FIG. 5. Spectral-angular distributions of SPR from the reference grating made of ten single copper particles (black curves) with a radius of 189 μm and from a grating made of ten dimers of interacting identical copper particles with a radius of 150 μm (red curves). Here, $\gamma = 50$ and $\varphi = 0$. (a) The black curve is multiplied by a factor of 40, $d = 6$ mm, $R = 517.8$ μm, $h = 2$ mm, and $\theta = 34.7°$. (b) $d = 7$ mm, $R = 552.7$ μm, $h = 3$ mm, and $\theta = 47.7°$. (c) Same as in Fig. 5(b) for $R = 907$ μm; (d) same as in Fig. 5(b) for $R = 990$ μm.

higher, while the first diffraction order becomes 1.5 times lower.

Figure 5(b) shows the same as in Fig. 5(a) for other parameters of the gratings. Here, the fourth diffraction order becomes 13 times higher, the fifth diffraction order becomes two times lower, and the third diffraction order almost does not change its height. Choosing another R value and keeping all other parameters, it is possible to enhance another diffraction order. For example, for the parameters in Fig. 5(b), choosing $R = 907\,\mu m$, we find [see Fig. 5(c)] that the fifth diffraction order becomes 10.5 times higher, while the fourth one becomes two times lower and the third one stays almost the same height. Figure 5(d) shows the same as Fig. 5(b) and (c), but for another value of R ($R = 990\,\mu m$). This value is out of resonant condition, so we see that the impact of the presence of dimers on the radiation spectra is almost negligible.

The resonant conditions considered here realize quasi-BICs, and it is precisely quasi- rather than real BICs, because, as we see, these conditions describe essentially radiative phenomena.

VIII. LONGITUDINAL INTERACTION

The previous theory does not include the influence of the interaction between the particles from different dimers, i.e., the interaction in the direction longitudinal to the electron's trajectory. Taking this interaction into account is a separate, intricate problem. Placing dimers far from each other, i.e., choosing a large period of the grating, does not help one avoid interdimer interactions, as the field of radiation from interacting particles harmonically depends on the distance between them with the period close to kd. The period chosen for plotting Fig. 5 suppresses the influence of the longitudinal interaction at enhanced maxima in order to show the pure effect. However, the longitudinal interaction is not necessarily a negative effect, as it can cause the highest degree of enhancement of radiation.

In the formulas obtained in Sec. II, the particular positions of the particles are not specified. Indeed, they contain the radius vectors $\mathbf{R}_1$ and $\mathbf{R}_2$, which allow one to consider different configurations defining $\mathbf{R}_1$ and $\mathbf{R}_2$ explicitly. In order to investigate the influence of the longitudinal interaction on the radiation properties, let us consider two particles placed along the electron trajectory, i.e., let the distance between them be d, the y coordinate for both of them to be equal to $R/2$, which means they are shifted to one side from the trajectory's projection. The field of radiation emitted in this case is defined by Eq. (2), while the spectral-angular distribution of radiation is defined by Eq. (20) for $m = 1$ (a single dimer).

Figure 6 demonstrates the wavelength dependence of the spectral-angular distribution of radiation. The black curves are plotted as if there is no longitudinal interaction, while the red curves take it into account. The curves in Fig. 6(a) and 6(b) are plotted for the parameters used in Fig. 5(a) and 5(b), respectively. The vertical dashed lines mark the positions of Smith-Purcell diffraction orders; the gray areas correspond to their width. The longitudinal interaction is seen to contribute around $\frac{1}{6}$ to $\frac{1}{8}$ compared with unity, and therefore in the first
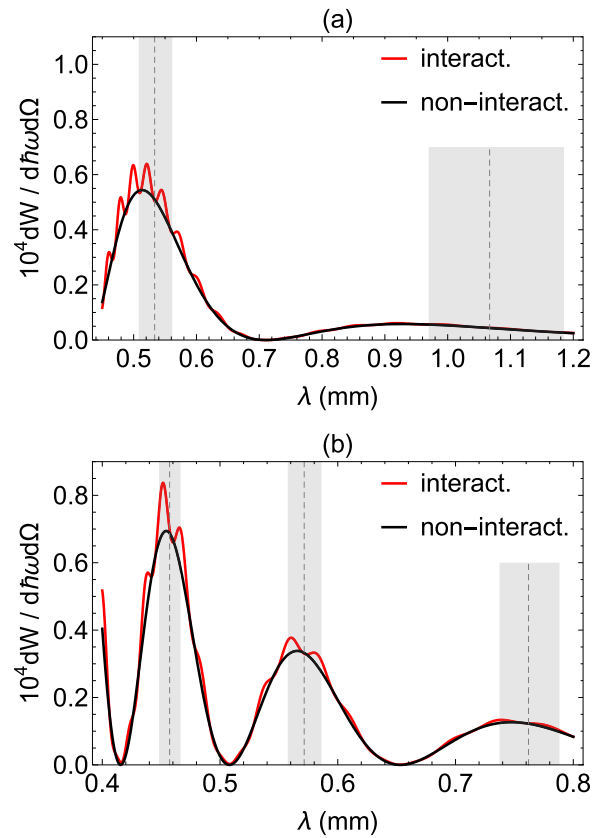

FIG. 6. The influence of longitudinal interaction. The wavelength dependence of the spectral-angular distribution of radiation from two particles with (red curves) and without (black curves) taking into account the interaction for the parameters of (a) Fig. 5(a) and (b) Fig. 5(b). The particles are placed along the electron trajectory. The vertical dashed lines mark the positions of SP diffraction orders; the gray areas correspond to their width.

approximation can be neglected for such periods d and a THz frequency range.

IX. SPECTRAL AND ANGULAR DISTRIBUTIONS

The previous formulas describe the spectral and angular distributions of radiation. These distributions bring the most detailed information about the intensity of radiation. Using them, we can obtain some other distributions.

Using the asymptotic formula

$$\frac{\sin^2\left[N\frac{d}{2}\left(\frac{\omega}{v} - k_x\right)\right]}{\sin^2\left[\frac{d}{2}\left(\frac{\omega}{v} - k_x\right)\right]} \xrightarrow{N \gg 1} 2\pi N \sum_s \delta\left[d\left(\frac{\omega}{v} - k_x\right) - 2\pi s\right],$$

$$(31)$$

where s is an integer and δ is the Delta function, we obtain

$$\frac{dW(\varphi, \omega)}{d\omega d\varphi} = \frac{\lambda}{d}Nc \int_0^\pi d\theta \sum_{s=s_1}^{s_2} \frac{\sin\theta}{|V|^2} |[\mathbf{k} \times (\mathbf{k} \times \mathbf{P})]|^2$$

$$\times \delta(\cos\theta - \beta^{-1} + s\lambda/d), \qquad (32)$$

where θ is the angle between the wavevector **k** and the x-axis ($n_x = \cos\theta$), and the limits of the sum are defined as

$$s_1 = \text{ceiling}[(\beta^{-1} - 1)d/\lambda],$$
$$s_2 = \text{floor}[(\beta^{-1} + 1)d/\lambda], \qquad (33)$$

with floor $[x]$ being the greatest integer less than or equal to x and ceiling $[x]$ being the smallest integer greater than or equal to x. These values come from a limitation of cosine and the fact that s must be an integer. So, after integration, we have

$$\frac{dW(\varphi,\omega)}{d\omega d\varphi} = \frac{\lambda}{d}Nc \sum_{s=s_1}^{s_2} \frac{1}{|V|^2} |[\mathbf{k}\times(\mathbf{k}\times\mathbf{P})]|^2 \Big|_{\cos\theta \to \beta^{-1} - s\lambda/d}.$$
$$(34)$$

The Delta function in Eq. (31) works also for determining the angular distribution of enhanced SPR. There are frequencies that give additional sharp maxima in spectral-angular distribution due to interaction, and they must be taken into account (for a description of how it works in detail, see, for example, Ref. [24]). Interestingly, however, under the condition of a resonance, i.e., when the frequency of separate Smith-Purcell diffraction orders coincides with that of interactions between particles, these additional frequencies will be taken into account automatically. Thus, we have

$$\frac{dW(\mathbf{n})}{d\Omega} = \frac{2\pi c}{d(\beta^{-1} - n_x)}Nc \int_{\omega_1}^{\omega_2} d\omega \sum_{s=s_1}^{s_2} |[\mathbf{k}\times(\mathbf{k}\times\mathbf{P})]|^2$$
$$\times \frac{1}{|V|^2}\delta\left[\omega - \frac{2\pi sc}{d(\beta^{-1} - n_x)}\right], \qquad (35)$$

where the limits of the sum are defined as follows:

$$s_1 = \text{ceiling}[(\beta^{-1} - n_x)d/\lambda_1],$$
$$s_2 = \text{floor}[(\beta^{-1} - n_x)d/\lambda_2], \qquad (36)$$

where $\lambda_{1,2} = 2\pi c/\omega_{1,2},$, and we have used Eq. (31). So, after integration in Eq. (35) over frequencies, we finally obtain

$$\frac{dW(\mathbf{n})}{d\Omega} = \frac{2\pi c}{d(\beta^{-1} - n_x)}Nc \sum_{s=s_1}^{s_2} \left|\frac{(\mathbf{k}\times(\mathbf{k}\times\mathbf{P}))}{V}\right|^2 \Big|_{\omega \to \omega^*}, \quad (37)$$

where $\omega^* = 2\pi sc/[d(\beta^{-1} - n_x)]$.

Figure 7 shows the spectral and angular distributions of SPR from a grating with the parameters corresponding to those in Fig. 5(a) (red curves, dimers) and the reference grating (black curves, chain).

While the spectral distribution of SPR from the reference grating monotonously decreases, the one from a grating of dimers has a maximum at the wavelength of interaction between particles in a dimer. Thus, the spectral distribution may become an additional source of information about the character of particles' interaction and, consequently, the grating or the dimer parameters.

On the contrary, the angular distributions of SPR from the gratings differ only in the amplitude, but not in the form. Note that the aliasing of all the curves in Fig. 7(a) originates from finite limits of integration. For example, integration in Eq. (35) over all frequencies would result in a smooth curve for SPR from the reference grating.
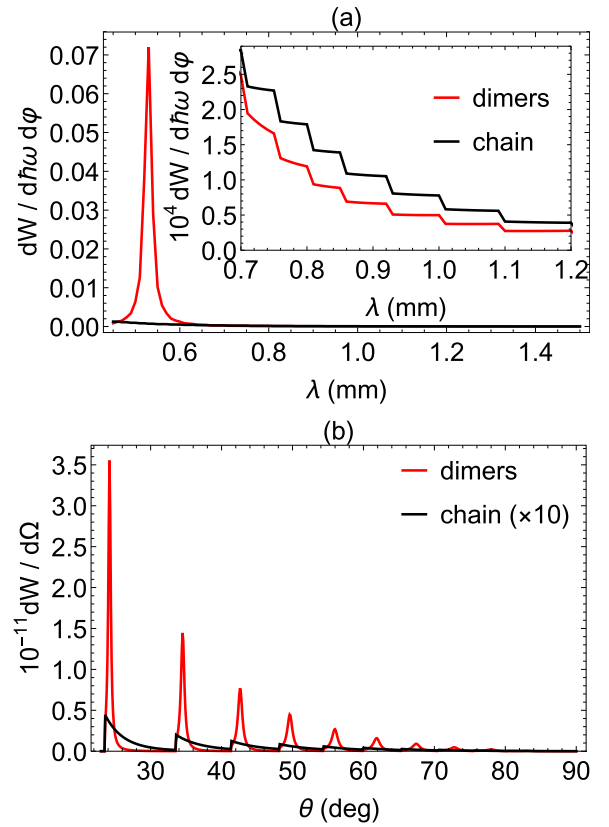

FIG. 7. (a) The spectral [see Eq. (34)] and (b) the angular [Eq. (35)] distributions of SPR. The parameters are the same as in Fig. 5(a). The black curve in Fig. 7(b) is multiplied by a factor of ten.

Figure 7(b) shows a very clear enhancement of the intensity of radiation in a spectral domain due to implementing quasi-BIC resonance—actually, about two orders of magnitude.

X. RANGE OF VALIDITY

In this section, we summarize all used approximations and the restrictions on parameters necessary for the theory to be correct.

The theory given previously is formulated in the dipole approximation, i.e., it is valid for small particles with the characteristic sizes $r_{1,2}$ much smaller than the wavelength of radiation:

$$r_1, r_2 \ll \lambda. \qquad (38)$$

The general restriction for effective emitting SPR follows from the effective radius of the electron's Coulomb field $\gamma\beta\lambda/2\pi$. The impact parameter h should be smaller or of the order of this radius:

$$h \leqslant \gamma\beta\lambda/2\pi. \qquad (39)$$

Also, there is an evident limitation. The distance between the centers of two spherical particles R cannot be less than the sum of their radii:

$$R \geqslant r_1 + r_2. \qquad (40)$$

Besides that, the minimal distance between the particles is limited to the possibility of classical consideration. When the

particles are at only a subnanometer distance, the quantum effects of tunneling take place, which leads to considerable changes in the electromagnetic properties of dimers [25,26].

When talking about enhancement, we compare the grating of dimers with the reference grating of single particles with greater volume. To avoid enhancement due to the shortening of the impact parameter, we considered the case when

$$h \gg R/2. \qquad (41)$$

The period of the grating was chosen such that the longitudinal interaction between the particles is suppressed. However, in practice, this limitation as well as that given by Eq. (41) is not necessary. Violation of these limitations could, in principle, lead to enhancement in the radiation intensity, but it needs additional calculations, which, possibly, would also require consideration of plasmons running along the chain, which goes beyond the scope of this work, although our qualitative estimates in Sec. VIII can be considered a first step in constructing the analytical theory of this class of phenomena.

Electron velocity was taken to be constant, which responses the small losses on radiation compared with the kinetic energy of the electrons. It is usual limitation in the problems of polarization radiation, correct when electrons are fast enough, and it allows considering both ultra- and nonrelativistic electrons.

XI. CONCLUSION

We have constructed a theory describing the generation of electromagnetic radiation occurring when a chain of resonant dimers is excited by the Coulomb field of electrons traveling along it. These resonances realize a particular case of BICs. We proved that the interaction between constituent particles of the chain leads to significant enhancement of Smith-Purcell radiation at resonant frequencies, and we have obtained the conditions describing this effect.

As was demonstrated, there is a wide range of parameters, for which it is possible to enhance individual SPR maxima up to two orders of magnitude. Apparently, the effect can be even stronger with the appropriate choice of parameters.

The parameters of the considered gratings are feasible. They can be produced, for example, by the electroplating method followed by direct laser imaging and etching. (In Ref. [27], we manufactured and explored a similar grating, but it was not resonant and it was arranged as a two-dimensional grating rather than the one-dimensional grating presented here.) As the spectral widths of the maxima defining the interaction are large enough (from 20 μm for chosen parameters), there is no need in high-accuracy placement of the particles constituent for the dimers to observe the enhancement of the radiation due to the interaction. Also, for the analysis, the dimer was constructed using two identical particles. Taking particles with different polarizabilities or different sizes, it is possible to control the resonant frequency and, thus, separate radiation peaks.

[1] J. von Neumann and E. P. Wigner, Über merkwürdige diskrete Eigenwerte, Physikalische Zeitschrift **30**, 465 (1929).

[2] E. N. Bulgakov and A. F. Sadreev, Self-trapping of nanoparticles by bound states in the continuum, Phys. Rev. B **106**, 165430 (2022).

[3] K. L. Koshelev, Z. F. Sadrieva, A. A. Shcherbakov, Yu. S. Kivshar, and A. A. Bogdanov, Bound states in the continuum in photonic structures, Phys. Usp. **66**, 494 (2023).

[4] V. V. Klimov, Optical nanoresonators, Phys. Usp. **66**, 263 (2023).

[5] N. M. Shubin, V. V. Kapaev, and A. A. Gorbatsevich, Bound states in the continuum in a quantum-mechanical waveguide with a subwavelength resonator, JETP Lett. **116**, 205 (2022).

[6] Z.-G. Chen, C. Xu, R. Al Jahdali, J. Mei, and Y. Wu, Corner states in a second-order acoustic topological insulator as bound states in the continuum, Phys. Rev. B **100**, 075120 (2019).

[7] N. K. Zhevago and V. I. Glebov, Modified theory of Smith-Purcell radiation, Nucl. Instrum. Methods. Phys. Res. Sect. A **341**, ABS101 (1994).

[8] M. I. Ryazanov, M. N. Strikhanov, and A. A. Tishchenko, Local field effect in diffraction radiation from a periodical system of dielectric spheres, Nucl. Instrum. Methods. Phys. Res. Sect. B **266**, 3811 (2008).

[9] Y. Yang, A. Massuda, C. Roques-Carmes, S. E. Kooi, T. Christensen, S. G. Johnson, J. D. Joannopoulos, O. D. Miller, I. Kaminer, and M. Soljačić, Maximal spontaneous photon emission and energy loss from free electrons, Nat. Phys. **14**, 894 (2018).

[10] Y. Song, N. Jiang, L. Liu, X. Hu, and J. Zi, Cherenkov radiation from photonic bound states in the continuum: Towards compact free-electron lasers, Phys. Rev. Appl. **10**, 064026 (2018).

[11] Z. Chen, L. Mao, M. Jin, and X. Shi, Improved Smith–Purcell free-electron laser based on quasi-bound states in the continuum, J. Phys. D Appl. Phys. **56**, 035101 (2023).

[12] Z. Chen, M. Jin, L. Mao, X. Shi, N. Bai, and X. Sun, Enhancement of Smith–Purcell radiation from cylindrical gratings by quasi-bound states in the continuum, Opt. Lett. **47**, 2911 (2022).

[13] Z. Chen, L. Mao, R. Yang, M. Jin, N. Bai, and X. Sun, Effect of absorption loss on resonance-enhanced Smith–Purcell radiation from metal-plate arrays, JOSA B **40**, 115 (2023).

[14] A. A. Tishchenko and D. Yu. Sergeeva, Near-field resonances in photon emission via interaction of electrons with coupled nanoparticles, Phys. Rev. B **100**, 235421 (2019).

[15] I. D. Morokhov, V. I. Petinov, L. I. Trusov, and V. F. Petrunin, Structure and properties of fine metallic particles, Sov. Phys. Usp. **24**, 295 (1981).

[16] H. Ehrenreich and H. R. Philipp, Optical properties of Ag and Cu, Phys. Rev. **128**, 1622 (1962).

[17] W.-F. Sun, X.-K. Wang, and Y. Zhang, Measurement of refractive index for high reflectance materials with terahertz time domain reflection spectroscopy, Chin. Phys. Lett. **26**, 114210 (2009).

[18] Y. Mou, Z.-S. Wu, Y.-Q. Gao, Z.-Q. Yang, Q.-J. Yang, and G. Zhang, Determination of the complex refractivity of Au, Cu and Al in terahertz and far-infrared regions from reflection spectra measurements, Infrared Phys. Technol. **80**, 58 (2017).

[19] J. Orosco and C. F. M. Coimbra, On a causal dispersion model for the optical properties of metals, Appl. Optics **57**, 5333 (2018).

[20] G. F. Bohren and D. R. Huffman, *Absorption and Scattering of Light by Small Particles* (Wiley, New York, 1983).

[21] E. J. Zeman and G. C. Schat, An accurate electromagnetic theory study of surface enhancement factors for Ag, Au, Cu, Li, Na, AI, Ga, In, Zn, and Cd, J. Phys. Chem. **91**, 634 (1987).

[22] M. A. Ordal, Robert J. Bell, R. W. Alexander, Jr, L. L. Long, and M. R. Querry, Optical properties of fourteen metals in the infrared and far infrared: Al, Co, Cu, Au, Fe, Pb, Mo, Ni, Pd, Pt, Ag, Ti, V, and W, Appl. Optics **24**, 4493 (1985).

[23] M. A. Ordal, L. L. Long, R. J. Bell, S. E. Bell, R. R. Bell, R. W. Alexander, and C. A. Ward, Optical properties of the metals Al, Co, Cu, Au, Fe, Pb, Ni, Pd, Pt, Ag, Ti, and W in the infrared and far infrared, Appl. Optics **22**, 1099 (1983).

[24] A. A. Savchenko, D. Y. Sergeeva, A. A. Tishchenko, and M. N. Strikhanov, Small-angle x-ray transition radiation from multi-layered structures, Phys. Rev. D **99**, 016015 (2019).

[25] K. J. Savage, M. M. Hawkeye, R. Esteban, A. G. Borisov, J. Aizpurua, and J. J. Baumberg, Revealing the quantum regime in tunnelling plasmonics, Nature (London) **491**, 574 (2012).

[26] P. Zhang, Scaling for quantum tunneling current in nano- and subnano-scale plasmonic junctions, Sci. Rep. **5**, 9826 (2015).

[27] D. Y. Sergeeva, A. S. Aryshev, A. A. Tishchenko, K. E. Popov, N. Terunuma, and J. Urakawa, THz Smith–Purcell and grating transition radiation from metasurface: Experiment and theory, Opt. Lett. **46**, 544 (2021).